Supporting Information

Concave PtCo nanooctahedra with high-energy {110} facets for oxygen reduction reaction

Zhijuan Li,[a] Xiaoru Wang,[a] Zhenbo Zhang,[a] Jinrui Hu[a], Zhenyuan Liu,*[ab] Dongmei Sun,[a] and Yawen Tang*[a]

[a] Jiangsu Key Laboratory of New Power Batteries, Jiangsu Collaborative Innovation Center of Biomedical Functional Materials, School of Chemistry and Materials Science, Nanjing Normal University, Nanjing 210023, P. R. China. E-mail: tangyawen@njnu.edu.cn.

[b] School of Materials Science and Engineering, Jiangsu University of Science and Technology, Zhenjiang 212003, P. R. China. E-mail: zhenyuanliu163@163.com.

Part I: Experimental section

Reagents and chemicals

Hexachloroplatinic(IV) acid hexahydrate ($H_2PtCl_6 \cdot 6H_2O$) was purchased from Shanghai Dibai Biotechnology Co., Ltd. Cobalt(II) chloride hexahydrate ($CoCl_2 \cdot 6H_2O$), Iminodiacetic acid ($C_4H_7NO_4$), and polyvinylpyrrolidone (PVP, Mw = 30,000) were purchased from Sinopharm Chemical Reagent Co., Ltd. (Shanghai, China). Commercial Pt black was purchased from Johnson Matthey Corporation. All reagents were of analytical reagent grade and used without further purification.

Synthesis of PtCo concave nanooctahedra (CNO)

In a typical synthesis, 0.5 mL of 0.05 M $H_2PtCl_6 \cdot 6H_2O$ solution, 0.5 mL of 0.05 M $CoCl_2 \cdot 6H_2O$ solution and 150 mg iminodiacetic acid were added into 9.0 mL deionized water and stirred for 30 min at room temperature. Then, 400 mg PVP polymer was added into above mixture solution with another continuous stir for 30 min. The resulting solution was transferred to a 25 mL Teflon-lined stainless steel autoclave and heated at 200 °C for 4 h. After being cooled to room temperature, the products were separated by centrifugation at 15000 rpm for 5 min and further purified by washing three times with ethanol and acetone. For comparison, pure Pt nanoparticles were also prepared using the same synthetic process without $CoCl_2 \cdot 6H_2O$ solution.

Physical characterization

The morphology of the samples were determined by a JEOL JEM-2100F transmission electron microscopy operated at 200 kV, which is used to performing transmission electron microscopy (TEM), high-resolution TEM (HRTEM) and selected area diffraction (SAED). High-angle annular dark-field scanning TEM (HAADF-STEM), energy dispersive spectrum

(EDS), energy dispersive X-ray (EDX) line scanning and elemental mapping measurements were performed on an FEI Tecnai G2 F20 microscope, which was built as an accessory on the JEOL JEM-2100F. Scanning electron microscopy (SEM) images were taken on a JSM-2010 microscopy at an accelerating voltage of 20 kV. X-ray diffraction (XRD) patterns were obtained with a Model D/max-rC X-ray diffractometer using Cu Kα radiation source (λ = 1.5406 Å) and operating at 40 kV and 100 mA. X-ray photoelectron spectroscopy (XPS) measurements were carried out on a Thermo VG Scientific ESCALAB 250 spectrometer with an Al Kα radiator, and the vacuum in the analysis chamber was maintained at about 10^{-9} mbar. The binding energy was calibrated by means of the C 1s peak energy of 284.6 eV. Ultraviolet and visible spectroscopy (UV-vis) spectra were recorded at room temperature on a Shimadzu UV3600 spectrophotometer equipped with 1.0 cm quartz cells.

Electrochemical measurements

All electrochemical tests were performed on a CHI 760E electrochemical analyzer (Shanghai, Chenhua Co.) equipped with high-speed rotators from Gamry Instruments. A conventional three-electrode system was used, including a rotating disk electrode (RDE) or rotating ring-disk electrode (RRDE) as the working electrodes (0.196 cm^{-2}, the inner diameter of the ring electrode is 6 mm and the outer diameter is 7 mm of ring electrode), a graphitized rod as the auxiliary electrode, and a saturated calomel electrode (SCE) as the reference electrode. Prior to the electrode preparation, the samples were treated with UV irradiation (wavelength at 185 and 254 nm in air for 24 h) to remove the capping agent. Electrodes were prepared by drop-casting ink containing catalyst powder on a glassy carbon electrode. The catalyst ink was prepared by ultrasonically dispersing the mixture of 5 mg of catalyst, 0.8 mL deionized water and 0.1 mL ethanol, and 0.1 mL of 5 wt.% Nafion solution. Then 10 μL of the catalysts are

dropped on electrode and dried at room temperature. The oxygen reduction reaction activities of the catalysts were measured *via* the RDE voltammograms in a 0.1 M KOH electrolyte at a rotation rate of 1600 rpm and a scan rate of 5 mV s^{-1}. Before testing, O_2 was purged into the electrolyte for at least 30 min to saturate the electrolyte with O_2. All potentials in this work have been calibrated into the reversible hydrogen electrode (RHE). The percentage of peroxide species (HO_2^-%) and electron transfer number (*n*) are calculated by the following equations:

$$HO_2^-\% = \frac{200I_r}{NI_d + I_r} \qquad n = \frac{4NI_d}{NI_d + I_r}$$

where I_d is the disk current, I_r is the ring current, and *N* is the current collection efficiency of the Pt ring, which is determined to be 0.38.

For the accelerated durability tests (ADTs), we performed cyclic voltammetry (CV) and ORR polarization curves after sweeping 1000 cycles at a rate of 100 mV s^{-1} in an O_2-saturated 0.1 M KOH solution. Meanwhile, full-scale voltammogram between 0 and 1.2 V (*vs*. RHE) in N_2-saturated 0.1 M KOH solution were recorded periodically to track the degradation of Pt electrocatalyst.

Part II: Figures and tables

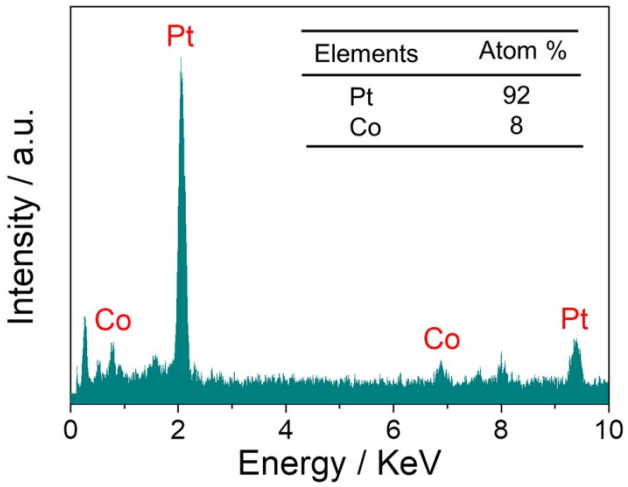

Fig. S1 EDS spectrum of the PtCo CNO.

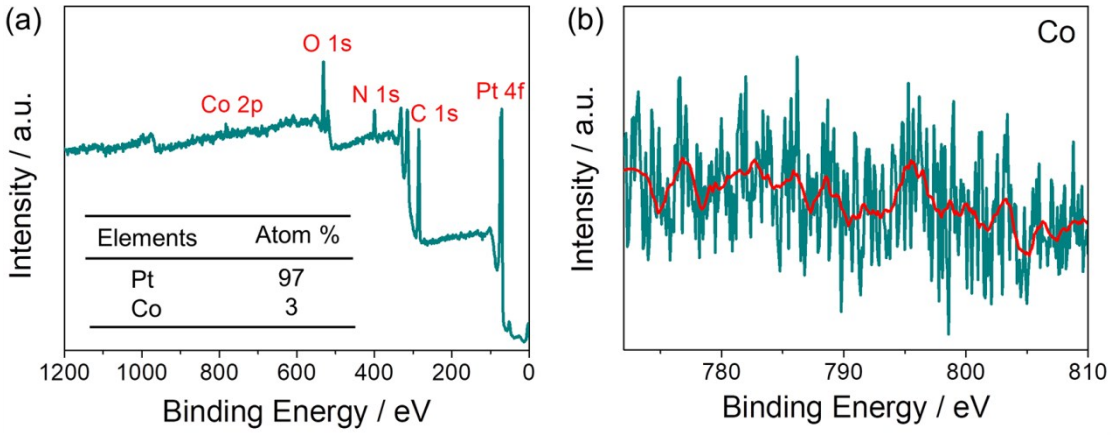

Fig. S2 (a) XPS survey scan spectrum of the PtCo CNO. (b) High-resolution XPS spectrum of Co 2p region in PtCo CNO.

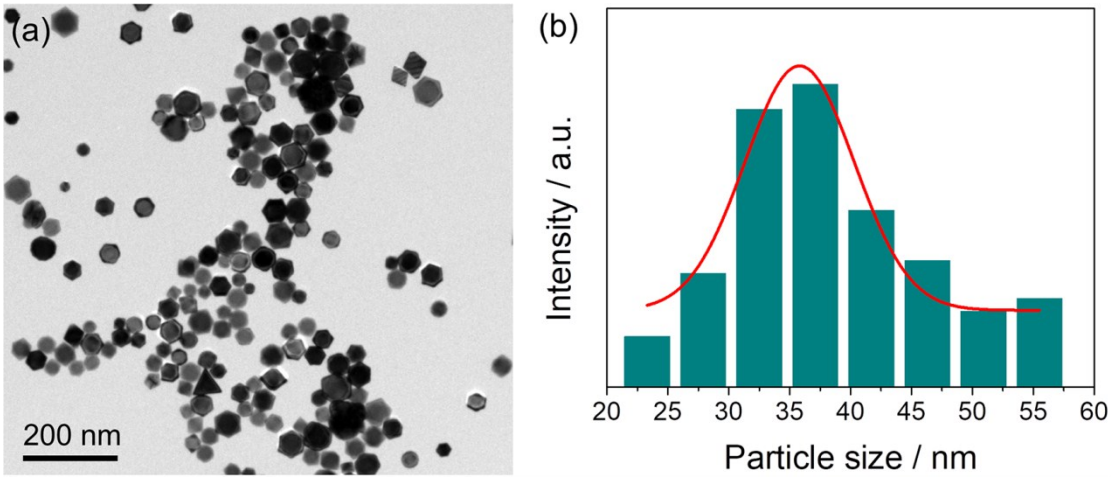

Fig. S3 (a) TEM image and (b) corresponding size histogram of the PtCo CNO.

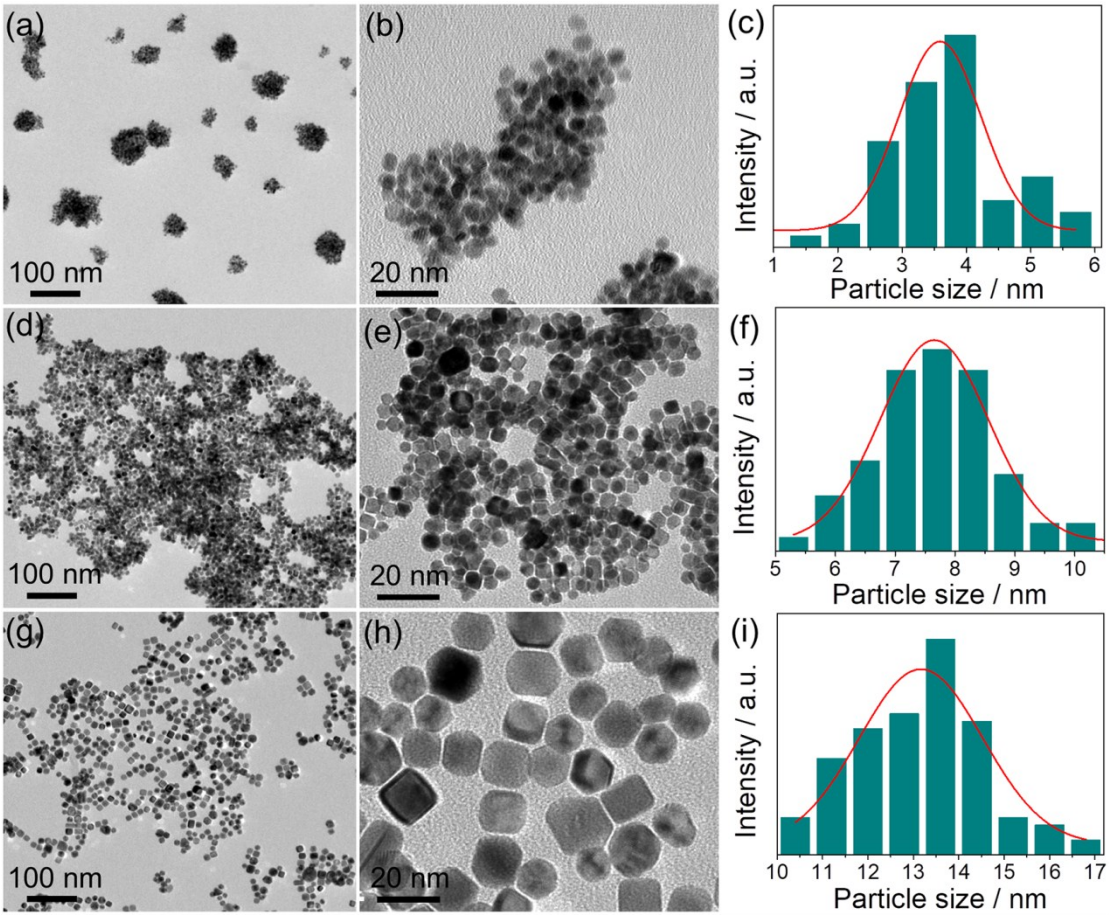

Fig. S4. TEM images and size histograms of PtCo nanoparticles with (a-c) 0 mg, (d-f) 30 mg and (g-i) 75 mg of iminodiacetic acid.

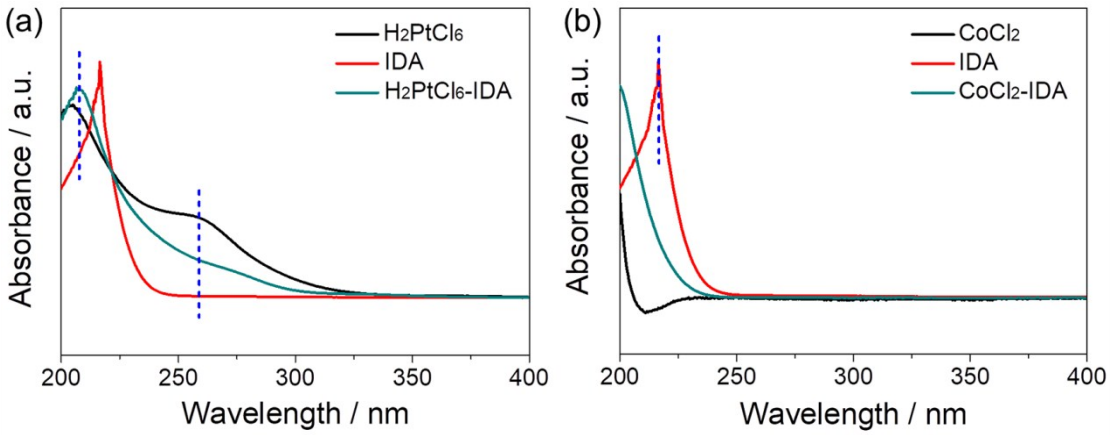

Fig. S5 (a) UV-vis spectra of the iminodiacetic acid solution, H_2PtCl_6 solution, and the mixed solution of iminodiacetic acid and H_2PtCl_6. (b) UV-vis spectra of the iminodiacetic acid solution, $CoCl_2$ solution, and the mixed solution of iminodiacetic acid solution and $CoCl_2$.

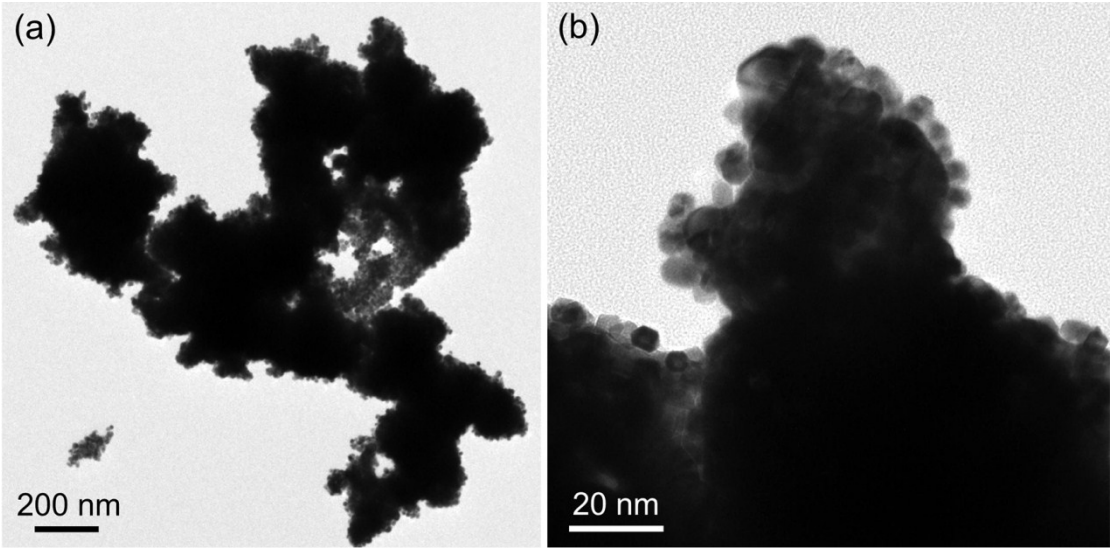

Fig. S6 TEM images of the prepared PtCo nanocrystals in the absence of PVP.

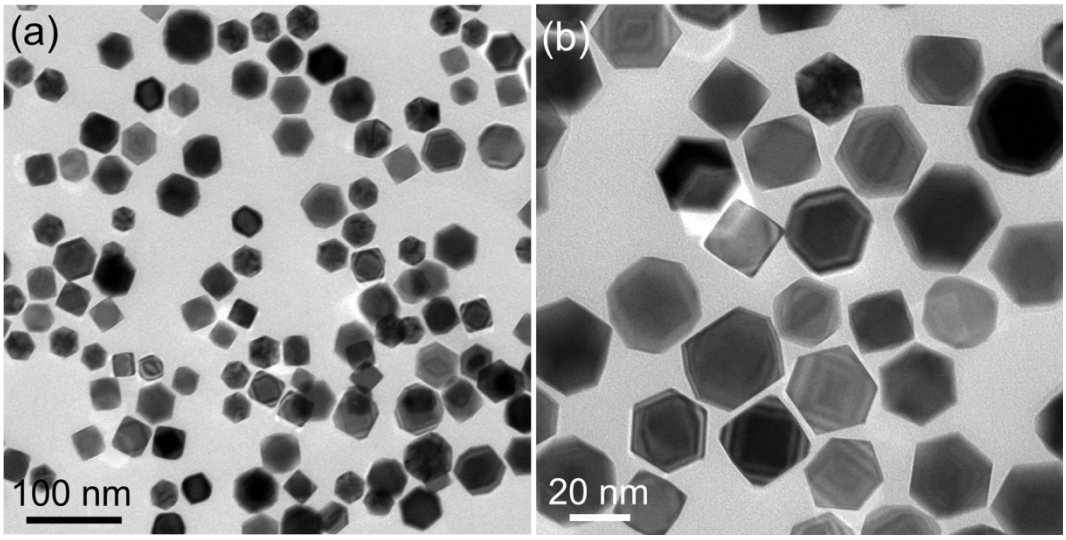

Fig. S7 TEM images of PtCo alloy nanocrystals prepared in the absence of Co^{2+}.

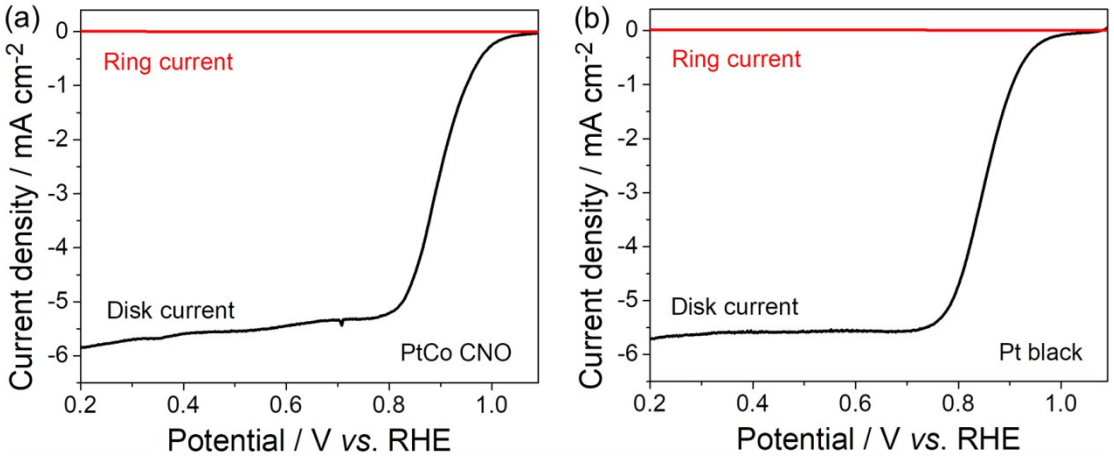

Fig. S8 The current collected on disk and ring electrodes catalyzed by (a) PtCo CNO and (b) Pt black.

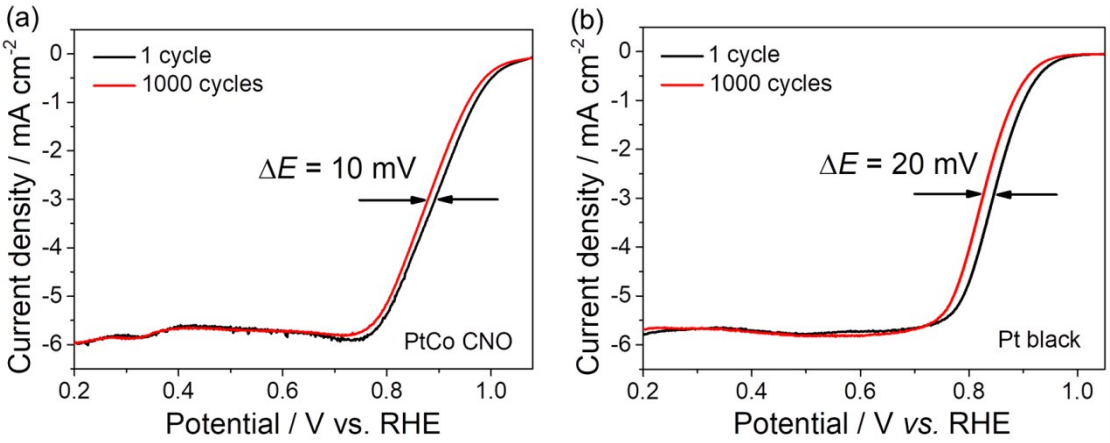

Fig. S9 ORR polarization curves of the (a) PtCo CNO and (b) Pt black before and after 1000 cycles in O_2-saturated 0.1 M KOH solution at a sweep rate of 5 mV s^{-1}.

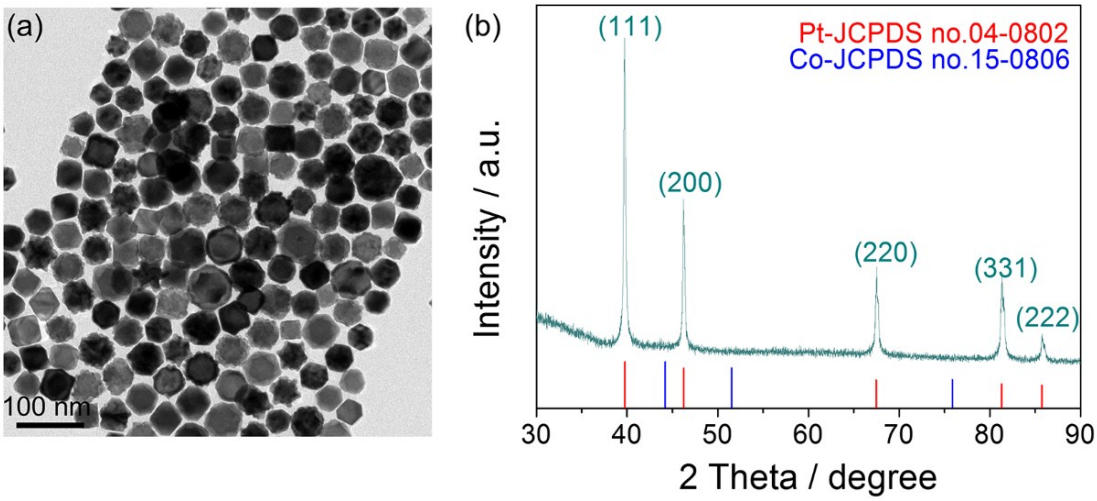

Fig. S10 (a) TEM image and (b) XRD pattern of the PtCo CNO after the stability test.

Table S1. Activity comparisons of PtCo CNO with the previous reported catalysts for the ORR in O_2-saturated 0.1 M KOH solutions at a rotation rate of 1600 rpm.

Catalyst	Onset potential (E_0/V)	Half-wave potential ($E_{1/2}$/V)	Ref.
PtCo CNO	1.02	0.89	this work
Pt NPs	1.00	0.86	this work
Pt black	0.99	0.85	this work
PtPd@Pt core/satellite nanoassemblies	0.98	0.88	[1]
Pt-Co/NC	N/A	0.87	[2]
$PtCo/CoO_xNCs$	N/A	0.86	[3]
Pt/MnO	N/A	0.78	[4]
PtPd nanosheets	1.0	0.88	[5]
PdPt Nanocubes	N/A	0.89	[6]
CuPt-TBTC/NGr-90	N/A	0.86	[7]
Pt-NB/G	N/A	0.86	[8]

References

1. Y. Chen, G. Fu, Y. Li, Q. Gu, L. Xu, D. Sun and Y. Tang, *J. Mater. Chem. A*, 2017, **5**, 3774-3779.
2. L.-L. Ling, W.-J. Liu, S.-Q. Chen, X. Hu and H. Jiang, *ACS Appl. Nano Mater.*, 2018, **1**, 3331-3338.
3. S. Hu, G. Goenaga, C. Melton, T. A. Zawodzinski and D. Mukherjee, *Appl. Catal.B: Environ.*, 2016, **182**, 286-296.
4. N. Zhang, L. Li, Y. Chu, L. Zheng, S. Sun, G. Zhang, H. He and J. Zhao, *Catal. Today*, 2019, **332**, 101-108.
5. H. Y. Chen, M. X. Jin, L. Zhang, A. J. Wang, J. Yuan, Q. L. Zhang and J. J. Feng, *J. Colloid Interf. Sci.*, 2019, **543**, 1-8.
6. K. Jukk, N. Kongi, K. Tammeveski, J. Solla-Gullón and J. M. Feliu, *ChemElectroChem*, 2017, **4**, 2547-2555.
7. R. Illathvalappil, V. M. Dhavale, S. N. Bhange and S. Kurungot, *Nanoscale*, 2017, **9**, 9009-9017.
8. S. Hussain, N. Kongi, L. Matisen, J. Kozlova, V. Sammelselg and K. Tammeveski, *Electrochem. Commun.*, 2017, **81**, 79-83.